*Journal of Power Sources*, 27 (1989) 155 - 165



# REAL-TIME CHARGE EFFICIENCY MONITORING AND ON-CHARGE GAS EVOLUTION IN TALL LEAD–ACID TRACTION CELLS

J. B. LAKEMAN

*Admiralty Research Establishment, Naval Engineering Department, West Drayton UB7 9BZ, Middlesex (U.K.)*

(Received March 12, 1989)

## Summary

The charging efficiencies of the positive and negative plates of the lead–acid traction cell can be determined by monitoring plate potential. This provides a precise and convenient method of assessing battery state-of-charge, battery health, and gas evolution levels. The charging efficiency of each plate is improved by electrolyte agitation, leading to a concomitant decrease in evolved gas.

## Introduction

The on-charge gas evolution, and associated charging efficiency, of lead–acid cells has received relatively scant attention in the literature [1 -4], and studies have not kept pace with technological advances in gas analysis instrumentation.

Knowledge of the charge efficiency (or charge acceptance) of lead–acid cells is of vital importance in determining the true state-of-charge and condition of the traction battery, and in the control of explosive gas mixtures. The development of a battery condition and battery health monitoring system is the subject of intensive research worldwide for various battery systems.

The charge efficiency, $X$, is the amount of charge stored relative to the amount being put into the battery by the battery charging system. This can be defined for both the positive and negative plates of the lead–acid cell in terms of the current going into gas evolution, $I_g$, and the current being delivered by the battery charger, $I$:

$$X = \frac{I - I_g}{I} \tag{1}$$

As lead–acid cells approach full charge, the charge efficiency progressively falls [2 - 4], making estimation of the total amount of charge stored uncertain. Knowledge of the charge efficiency during real-time operation

would minimise overcharge, facilitate the estimation of the true state-of-charge, and allow automatic detection of battery problems and the initiation of corrective responses.

It has so far proved difficult to determine charge efficiency accurately on a real-time basis during uninterrupted operation of lead–acid batteries. Charge efficiency estimates are not usually made and the state-of-charge assessment of the traction battery relies on the relatively crude arrangement of measuring the electrolyte specific gravity from the top of a few selected cells in a large battery. Changes in performance of individual cells are very difficult to detect.

Thus, a simple method for determining charge efficiencies during real-time operation would be extremely advantageous. This would enable predictions of battery state-of-health, state-of-charge, condition, and gas evolution levels to be made.

This work examines the feasibility of monitoring cell and plate potentials in order to estimate the charging efficiency using a standard Tafel expression to describe the gas evolution current

$$I_g = a \exp(bE) \tag{2}$$

at either or both electrodes. The empirical constants are conveniently measured or updated, without discharging the battery or cell, by measuring the plate potentials as a function of current when the cell is fully charged.

Using the charge efficiency, the true state-of-charge, $S$, of either battery or electrodes can be determined using

$$S(t) = \frac{C' - C - (\int XI\,dt)}{C'} \tag{3}$$

where $C$ is the charge taken out on the previous discharge and $C'$ is the rated capacity at that particular rate of discharge.

The effect of electrolyte agitation on charging efficiency and gas evolution was also investigated.

## Experimental

Eight 2 V lead–acid traction cells of 8400 A h nominal capacity were removed from a submarine at mid-service and connected in series. The performance of the cells was checked and found to be well within specified capacity.

The battery was then subjected to discharge/charge cycles. Charging was always carried out using a three-stage, constant current technique. The initial charging rate was 1900 A. This current was maintained until the battery voltage had risen to 19.2 V, when it was reduced to 900 A and the voltage was again allowed to rise to 19.2 V. The current was then reduced to 280 A and maintained until the battery voltage was constant over a 2 h period. The battery was discharged at one of three, constant current, rates: 1680 A, 940 A or 510 A.

The negative plate group voltages of each cell were continuously monitored by immersing a mercury/mercury(I) sulphate electrode in the electrolyte. Cell voltages were also measured and the positive plate group voltage was obtained from the difference.

Hydrogen and oxygen contents of the gases evolved from each cell were determined using a quadrupole mass spectrometer; the gas flow rate was measured using electronic mass flowmeters.

The constants of eqn. (2) were assessed by measuring steady-state cell and plate voltages of fully charged cells at currents of 80 - 400 A, assuming that all the current was being consumed in gas evolution at both plates. Measurements were carried out in the temperature range 20 - 25 °C with no electrolyte agitation.

The effect of electrolyte stratification on charge efficiency was examined by agitating the electrolyte in four of the cells on charge using the air pump method described by Bagshaw [5].

## Results and discussion

*(i) On-charge gas evolution data*

Figures 1 and 2 show typical cell potential and temperature plots *versus* time during the charge following a discharge at 940 A for cells with, and without, electrolyte agitation, respectively. Stages in the three-rate charging procedure are readily apparent in the potential plots, with rate changes at 4.05 h and 5.85 h and charge ending at 14.45 h. The top-of-charge potential is achieved earlier for cells charged with electrolyte agitation, indicating a superior charging efficiency. This phenomenon is also reflected in the plots of hydrogen and oxygen flow rates *versus* time, shown in Figs. 3 and 4, respectively. The plots shown are for the same cells during the same charge

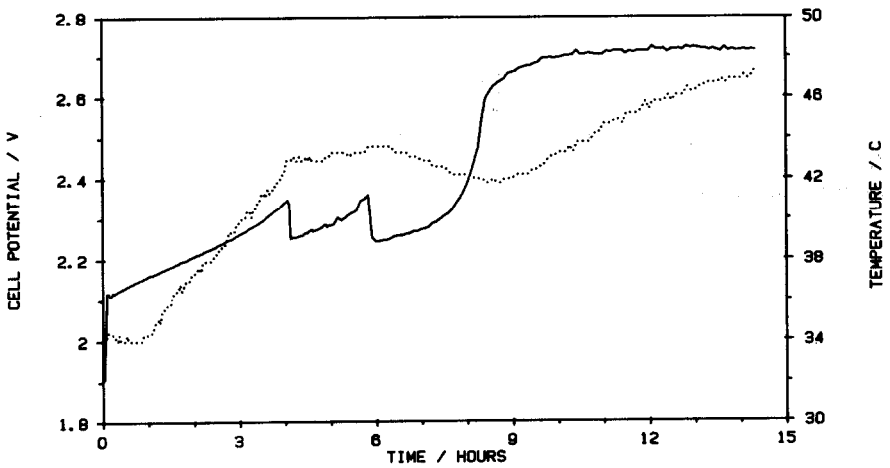


Fig. 1. Plot of cell voltage (——) and cell temperature in °C (·····) against time during charge following a discharge at 940 A. Cell charged without electrolyte agitation.

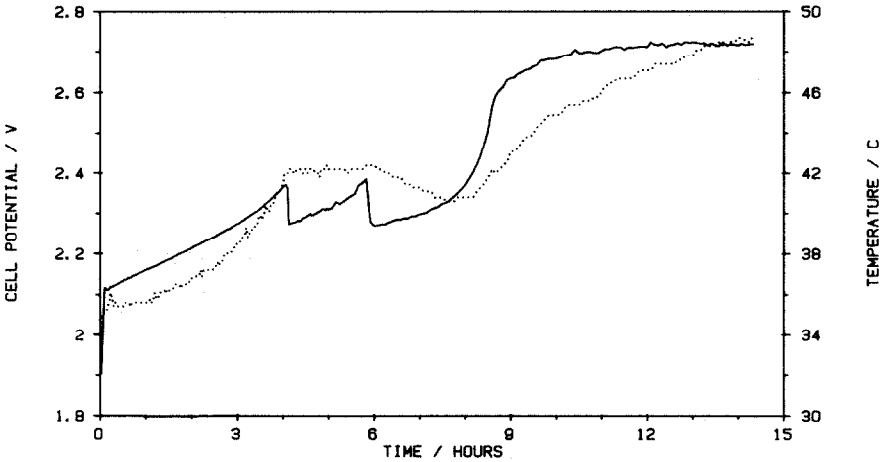


Fig. 2. Plot of cell voltage (——) and cell temperature in °C (·····) against time during same charge as Fig. 1. Cell charged with electrolyte agitation.

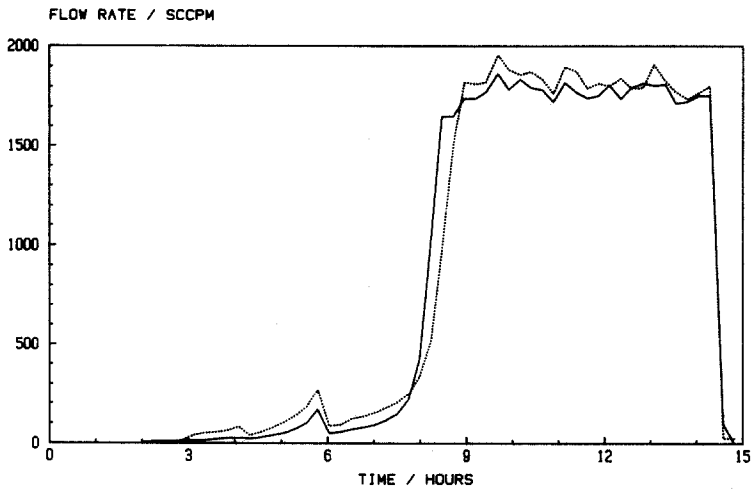


Fig. 3. On-charge hydrogen gas flow rate in standard cubic centimetres per minute (SCCPM) against time for cells charged with (——) and without (·····) electrolyte agitation following discharge at 940 A.

as Figs. 1 and 2. It is readily apparent that gas evolution at both negative and positive plates occurs to a significantly greater extent during the earlier stages of charge for cells being charged without electrolyte agitation. The final top-of-charge flow rate is, however, achieved more rapidly by cells being charged with electrolyte agitation. The amount of gas evolved during charge has a direct effect on charging efficiency (see eqn. (1)). It can be concluded that charging efficiency is improved and, hence, top-of-charge is reached more rapidly when cells are charged with electrolyte agitation in order to minimise electrolyte stratification [3]. Equation (3) was used to

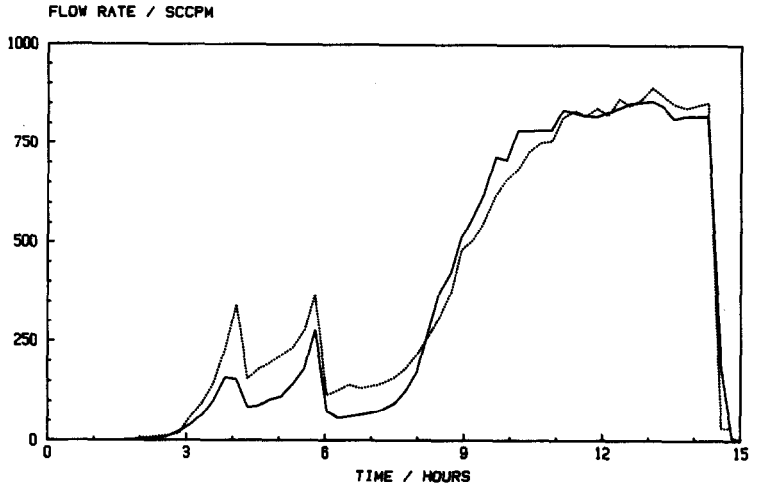


Fig. 4. On-charge oxygen flow rate against time for cells charged with (——) and without (·····) electrolyte agitation following discharge at 940 A.

calculate the times to full charge for the negative and positive plates of the cells depicted in Figs. 1 - 4:

| | |
|---|---|
| Negative plate, no agitation | 8.46 h |
| Negative plate, with agitation | 8.41 h |
| Positive plate, no agitation | 9.53 h |
| Positive plate, with agitation | 8.92 h |

Similar results were observed for charges following different rates of discharge, with electrolyte agitation effecting a more marked reduction in charge time at the positive than at the negative electrode. These charge times, and comparison of Figs. 3 and 4, also demonstrate that the charging efficiency of the positive plate is lower than that of the negative plate at early stages of charge. The charge efficiency and true state-of-charge *versus* time plots for the positive and negative plates of a cell charged with electrolyte agitation are shown in Figs. 5 and 6. Data shown are for the cell characterised in Figs. 2 - 4, and the parameters were calculated using eqns. (1) and (3). The negative plate was charged with high efficiency until full charge was reached, when the charge efficiency rapidly fell to a minimum as hydrogen evolution reached a maximum. The charge efficiency of the positive plate dropped progressively with increasing state-of-charge [2 - 4]. The early and progressive evolution of oxygen from the positive plate indicates the progressive nature of the conversion of the lead sulphate to lead dioxide. The conversion of lead sulphate to lead at the negative plate occurs in a more uniform manner.

The lower charging efficiency of the positive plate is also due to the fact that the charge/discharge reactions occur entirely within the potential region for oxygen evolution. The potentials, *versus* the mercury/mercury(I) sulphate reference electrode, at which the onset of gassing was first detected were found to be −1.07 V at the negative plate and 1.2 V at the positive

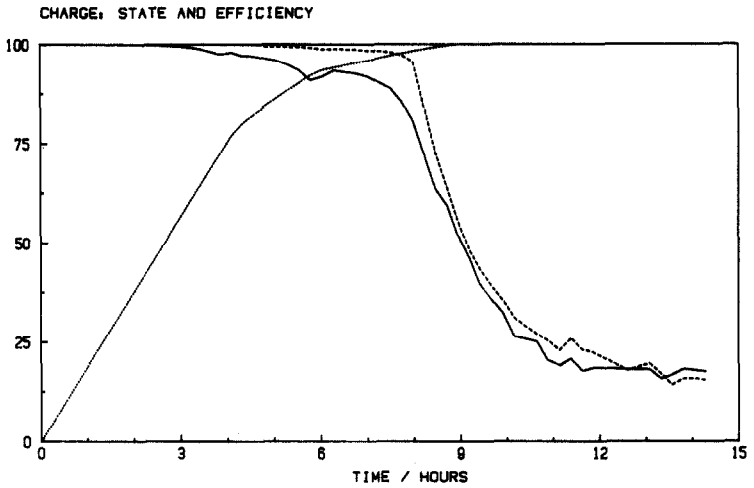


Fig. 5. Real state-of-charge (·····), experimental (——), and theoretical (- - - -) charge efficiencies *vs.* time plots, for positive plate group, of cell charged with electrolyte agitation following discharge at 940 A.

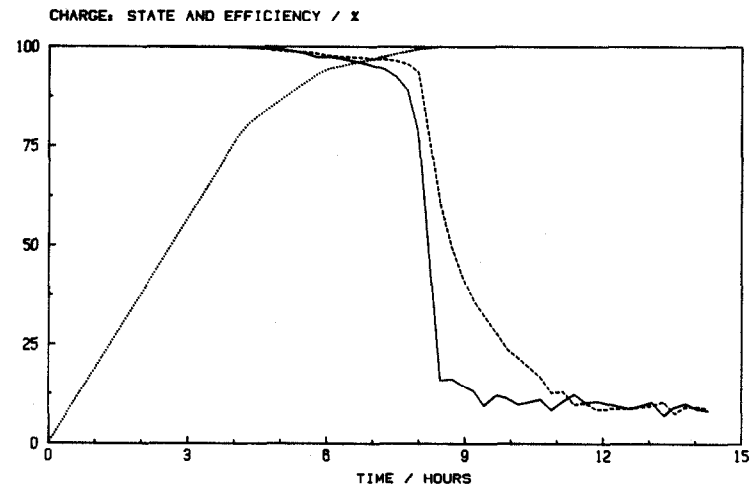


Fig. 6. Real state-of-charge (·····), experimental (——), and theoretical (- - - -) charge efficiencies *vs.* time plots, for negative plate group, of cell charged with electrolyte agitation following discharge at 940 A.

plate. It must be stressed, however, that the potentials measured are, effectively, the average potentials of electrodes of very large surface area.

The disparities in charge efficiency behaviour between the positive and negative plates highlight the problems of trying to estimate the state-of-charge and state-of-health of a battery from measurements of cell potential alone. Reliable data can only be arrived at from measurements of plate potentials.

Figures 5 and 6, and data from other charges, indicate that at top-of-charge, 90 - 95% of the charging current goes into hydrogen evolution at the

negative plate, but oxygen evolution at the positive plate is only about 85% efficient. The inefficiency of the negative plate could be due to oxygen recombination, whereas the inefficiency at the positive plate has been attributed to the production of persulphuric acid [2]. In the present work, however, no evidence was found for the evolution of oxygen from persulphate decomposition after the end of charge.

The differences in the gas evolution efficiencies at the positive and negative plates (see Figs. 5 and 6) are also reflected in the ratio of the volumes of hydrogen to oxygen evolved on charge. The on-charge gas evolution curves (see, for example, Figs. 3 and 4) were integrated to give the total volumes of hydrogen and oxygen evolved. The ratio of hydrogen to oxygen was calculated for each cell. No significant difference was found between the ratios calculated for cells charged with, and without, electrolyte agitation. Average ratios were calculated for the charges following different discharge rates. Following discharge rates of 510 A, 940 A and 1680 A, the average hydrogen to oxygen ratios were found to be 2.02, 2.16 and 2.17, respectively. These data suggest that the theoretical stoichiometric ratio is only approached as the depth of discharge is maximised. This is probably due to the effects of oxygen recombination, as more negative surface area is available for oxygen recombination as the rate of the previous discharge increases.

*(ii) Top-of-charge experiments*

Tafel plots were made from the data of top-of-charge experiments. The Tafel slope for hydrogen evolution was found to be in the range −0.177 V to −0.145 V with a mean of −0.159 V.

The Tafel slope for hydrogen evolution at a planar lead electrode in sulphuric acid has been reported as −0.12 V [6, 7]. The present slope suggests that the negative plate is porous and that hydrogen evolution is not restricted to the front face of the electrode.

The Tafel slope for oxygen evolution was found to be between 0.113 V and 0.131 V with a mean of 0.12 V. This value confirms other work on battery electrodes [4]. The same slope was, however, also measured on effectively planar lead dioxide electrodes [8], suggesting that the positive plate behaves as a planar electrode for oxygen evolution. One reason for this could be the tortuous nature of the pores in the positive plate as compared with the more open structure of the negative plate [9]. This would tend to lead to pore blocking by gas bubbles so that gas evolution only occurs unhindered at the front face of the electrode. This is confirmed by Barak *et al.* [10] who found that the effective surface area for oxygen evolution at the positive plate was only an order of magnitude greater than the nominal area.

Data from top-of-charge experiments were used to determine the constants of eqn. (2). $a$ and $b$ were found to be in the ranges 1.321E-7 to 6.79E-6 and 12.9 to 15.84, respectively, for the negative plate. For the positive plate, the ranges were 1.971E-11 to 7.892E-10 and 17.57 to 20.34, respectively.

*(iii) Estimating battery health/condition parameters*

Figure 7 shows the plate group potentials against time plots for the cell characterised in Figs. 2 - 6. These potentials, and the constants measured from top-of-charge data, were used, together with eqns. (1) and (2), to estimate theoretical charging efficiencies for the positive and negative plates. The results are shown in Figs. 5 and 6, respectively, where the theoretical predictions are compared with experimental data. Agreement between theory and experiment is very good and confirms that the true state-of-charge of a cell or battery can be estimated from simple plate group potential data.

Theoretical and experimental on-charge gas flow rates are plotted for the positive and negative plates in Figs. 8 and 9. Again, agreement between theory and experiment is, in general, excellent, although disparity between theory and experiment for the positive plate at early stages of charge is evident. This highlights the problem of using an average potential when gas is being evolved from a progressively greater electrode area as charge proceeds. It is evident, however, that dangerous gas levels and compositions could be predicted from simple plate group potential measurements.

Figures 8 and 9 also show gas flow rates estimated from the cell potential data of Fig. 2. In this case, although the hydrogen flow rate is underestimated compared with the plate potential data, and the oxygen flow rate is overestimated, the agreement between theory and experiment is still good under the controlled charging conditions used. In an uncontrolled charging regime, with no voltage limit, it is anticipated that the errors involved in using the cell potential data alone would be unacceptable.

Figure 10 shows the overall charge efficiency of the cell depicted in Figs. 2 - 9 plotted against time. The overall charge efficiency was calculated as the average of the measured negative and positive plate values. Also

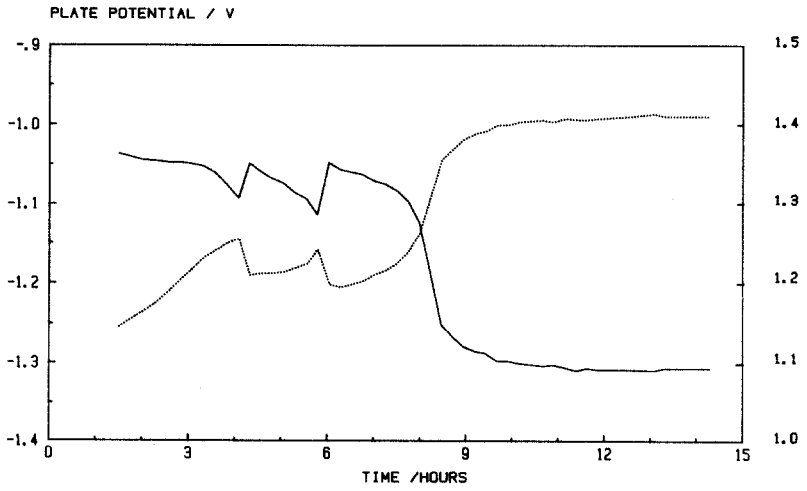


**Fig. 7. Negative (——, and left axis) and positive (·····, and right axis) plate group potential *vs.* time plots for cell charged following discharge at 940 A.**

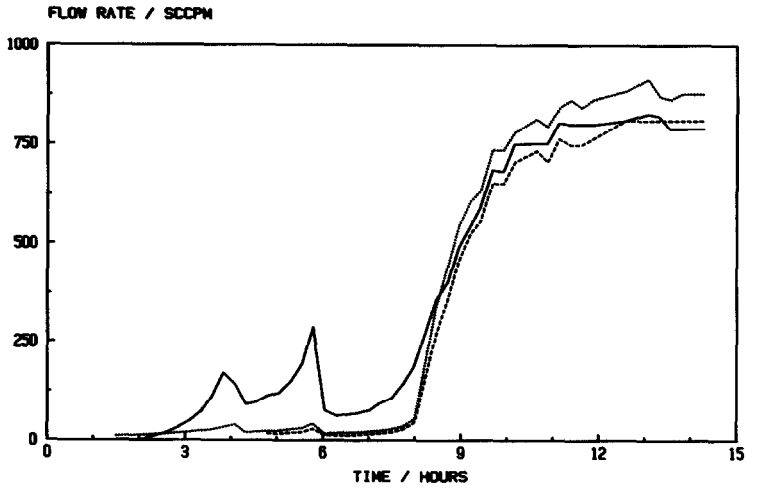


Fig. 8. On-charge oxygen gas flow rates against time for cell charged with electrolyte agitation following discharge at 940 A. Full line shows experimental data. Broken line shows theoretical data calculated from plate potential of Fig. 7 and constants of eqn. (2) where $a$ = 1.65E-10 and $b$ = 19.84. Dotted line shows theoretical data calculated from cell potential of Fig. 2 and constants of eqn. (2) where $a$ = 3.1E-8 and $b$ = 8.395.

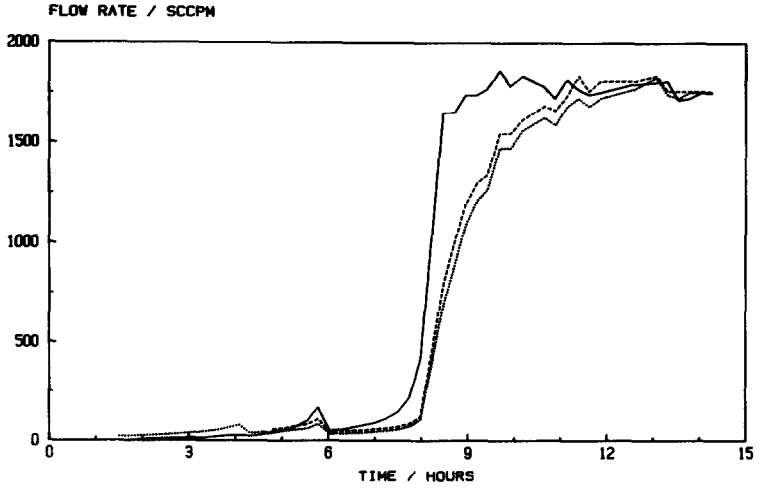


Fig. 9. On-charge hydrogen gas flow rates against time for cell charged with electrolyte agitation following discharge at 940 A. Full line shows experimental data. Broken line shows theoretical data calculated from plate potential of Fig. 7 and constants of eqn. (2) where $a$ = 1.723E-6 and $b$ = 14.387. Dotted line is for theoretical data calculated from cell potential as per Fig. 8.

shown, is the estimated state-of-charge calculated using the overall charge efficiency. These data should be compared with the theoretical data calculated from the cell potential data of Fig. 2 and shown in Fig. 11. The tendency is to overestimate the current efficiency at early stages of charge, but the current efficiency falls in a more progressive manner as the charge

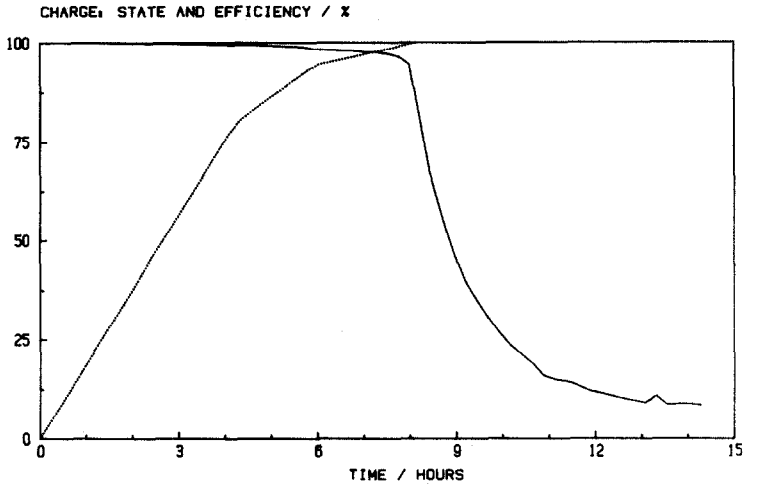


Fig. 10. Experimental overall charge efficiency and state-of-charge *vs.* time plots for cell of Figs. 2 - 9.

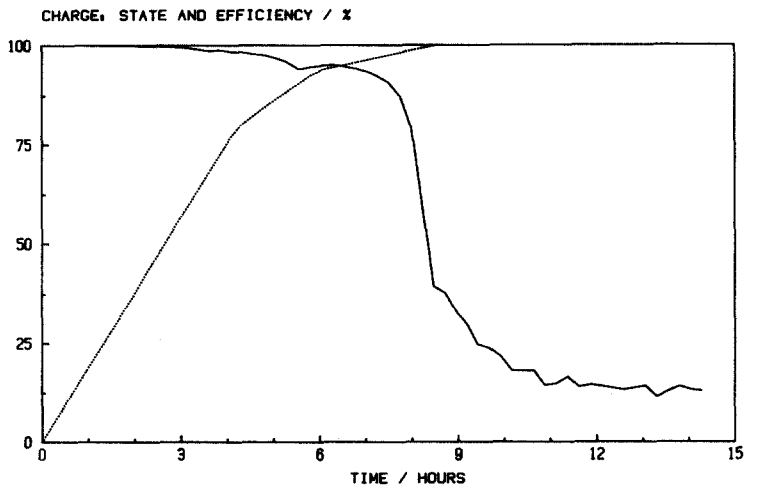


Fig. 11. Theoretical overall charge efficiency and state-of-charge *vs.* time plots for cell of Figs. 2 - 9.

proceeds. These trends are reflected in the theoretical gas evolution predictions of Figs. 8 and 9. The theoretical state-of-charge estimation of Fig. 11 is in good agreement with the measured data of Fig. 10, with a tendency to overestimate in line with the charge efficiency calcualtions. In a less-controlled charging regime with no voltage limit, however, charge efficiency will be significantly reduced at early stages of charge and will be different at each electrode. This will lead to unacceptable errors in the estimation of top-of-charge.

*(iv) Requirements for system application*

For the method evaluated here to be applied to a battery health/condition monitoring system, several requirements need to be met. Firstly, individual plate group potentials must be monitored and logged by a central processing facility. The system must also have the ability, periodically, to determine the overcharge voltage of each plate group as a function of current. This should be done when the battery is fully charged. The system could be fine-tuned by monitoring and adjusting for changes in temperature. In addition, an account should be kept by the central processor of the charge into and out of the battery.

## Conclusion

A method has been demonstrated which allows the charge efficiency of lead–acid cells to be monitored effectively in real time using only voltage measurements as inputs. With further development this method could be used to monitor the state-of-health, state-of-charge, and conditions of the batteries, of electrically powered vehicles.

## References


1 G. R. Webley, *Proc. 2nd Int. Symp. on Batteries, October 1960*, MOD Inter-departmental Committee on Batteries, U.K.
2 K. Peters, A. I. Harrison and W. H. Durrant, in D. H. Collins (ed.), *Power Sources 2*, Pergamon, Oxford, 1970, p. 1.
3 W. G. Sunu and B. W. Burroughs, in J. Thompson (ed.), *Power Sources 8*, Academic Press, London, 1981, p. 601.
4 W. Visscher, in L. Pearce (ed.), *Power Sources 10*, The Paul Press, London, 1985, p. 525.
5 N. E. Bagshaw, *Batteries in Ships*, Research Studies Press, Chichester, 1982, p. 106.
6 Z. A. Jafa, *Zh. Fiz. Khim., 19* (1945) 117.
7 B. N. Kabanov and S. Jofa, *Acta Physicochim. USSR, 10* (1939) 617.
8 J. Burbank, A. C. Simon and E. Willihnganz, in P. Delahaye and C. W. Tobias (eds.), *Advances in Electrochemistry and Electrochemical Engineering 6*, Wiley-Interscience, New York, 1971, p. 157.
9 K. Micka, M. Svata and V. Koudelka, *J. Power Sources, 4* (1979) 43.
10 M. Barak, M. Gillibrand and K. Peters, *Proc. 2nd Int. Symp. on Batteries, October 1960*, MOD Inter-departmental Committee on Batteries, U.K.